Journal of Power Sources 187 (2009) 627–634

Contents lists available at ScienceDirect

Journal of Power Sources

journal homepage: www.elsevier.com/locate/jpowsour

Experimental investigations of an ionic-liquid-based, magnesium ion conducting, polymer gel electrolyte

G.P. Pandey, S.A. Hashmi*

Department of Physics & Astrophysics, University of Delhi, Delhi 110007, India

ARTICLE INFO

Article history:
Received 9 July 2008
Received in revised form 3 September 2008
Accepted 16 October 2008
Available online 7 November 2008

Keywords:
Gel polymer electrolyte
Ionic liquid
Magnesium ion conductor
Magnesium batteries
AC impedance spectroscopy
Cyclic voltammetry

ABSTRACT

Studies on a novel magnesium ion conducting gel polymer electrolyte based on a room temperature ionic liquid (RTIL) is reported. It comprises a Mg-salt, $Mg(CF_3SO_3)_2$ [or magnesium triflate, $Mg(Tf)_2$] solution in an ionic liquid, 1-ethyl-3-methylimidazolium trifluoro-methanesulfonate (EMITf), immobilized with poly(vinylidene fluoride-hexafluoropropylene) (PVdF-HFP), which is a freestanding, semitransparent and flexible film with excellent mechanical strength. Physical and electrochemical analyses demonstrate promising characteristics of these films, suitable as electrolytes in rechargeable magnesium batteries. The material offers a maximum electrical conductivity of $\sim 4.8 \times 10^{-3}$ S cm^{-1} at room temperature (20 °C) with excellent thermal and electrochemical stabilities. Possible conformational changes in the polymer host PVdF-HFP due to ionic liquid solution entrapment and ion–polymer interaction are investigated by Fourier transform infra-red (FTIR), X-ray diffraction (XRD) and scanning electron microscopic (SEM) methods. The Mg^{2+} ion transport in the gel film is confirmed from cyclic voltammetry, impedance and transport number measurements. The Mg^{2+} ion transport number (t_+) is ~0.26, which indicates a substantial contribution of triflate anion transport along with ionic conduction due to the component ions of the ionic liquid.

1. Introduction

The need for high performance and environment-friendly rechargeable batteries is of a major global interest. Presently, worldwide attention is directed towards the development of advanced battery technologies based on lithium, though rechargeable lithium metal batteries with high specific capacities are still commercially unavailable. To date, the rechargeable lithium-ion battery has been one of the best choices in view of its specific capacity and cycle stability [1]. Nevertheless, lithium-ion batteries are relatively expensive and suffer from some safety limitations. Recently, the magnesium-based rechargeable battery system has attracted attention due to its performance capabilities that are close to those of lithium-based alternatives [1–3]. Magnesium is an attractive anode material for batteries of high specific energy because it has a low electrochemical equivalence (12.15 g equiv.$^{-1}$) and a considerably negative electrode potential (−2.3 V versus SHE). In addition, it is cost effective due to natural abundance and safer than lithium. The use of magnesium as a negative electrode in aqueous primary and rechargeable batteries has been reported [4]. Aurbach et al. [5] have recently developed a prototype rechargeable magnesium battery using electrolyte solutions with Mg organohaloaluminate salts. The same group has also examined Chevrel phases of Mo_6T_8 (T = S, Se) as practical cathode materials for rechargeable Mg batteries, in which Mg^{2+} ions can be inserted reversibly [6,7]. Despite these studies, the development of rechargeable Mg batteries has yet not accelerated mainly due to the irreversibility of the Mg negative electrode and the lack of suitable Mg^{2+} conducting, nonaqueous electrolytes [8]. Thus, the development of solid-state Mg^{2+} conducting electrolytes has become one of the key issues to realize rechargeable solid-state Mg batteries.

Gel polymer electrolyte films are frequently used as excellent substitutes for liquid electrolytes for flexible and solid-state electrochemical devices, e.g., batteries, and supercapacitors [9,10]. Such gel electrolytes, mostly reported for lithium systems, are generally prepared by mixing a polar organic solvent, salts, and a host polymer matrix [9,10]. Mg^{2+} conducting gel polymer electrolytes have not been widely reported except for a few systems with aprotic organic plasticizers such as ethylene carbonate (EC), propylene carbonate (PC), and diethyl carbonate (DEC) [11–13] or with gels based on PEO-Grignard with high ionic mobility [14]. A few solid-state rechargeable magnesium batteries using polymer gel electrolytes have also been investigated [15,16]. It has been widely accepted that polymer gel electrolytes possess some distinct advantages over liquid electrolytes, such as reduced reactivity, reduced leakage, improved safety, and better shape flexibility and manufacturing

* Corresponding author. Fax: +91 1127667061.
E-mail address: sahashmi@physics.du.ac.in (S.A. Hashmi).

0378-7753/$ – see front matter © 2008 Elsevier B.V. All rights reserved.
doi:10.1016/j.jpowsour.2008.10.112

integrity. On the other hand, low-molecular-weight organic solvents/plasticizers (e.g., PC, DEC, etc.) suffer from fast evaporation, which limits their thermal stability and electrical/electrochemical properties. Moreover, these organic solvents are also responsible for the narrower electrochemical window and working voltage range of devices based on polymer gel electrolytes [17]. Therefore, it is the area of current interest to develop gel polymer electrolytes that consist of non-volatile solvents with a wider potential window and better thermal and electrochemical properties.

In recent years, room temperature ionic liquids (RTILs) have been proposed as non-volatile polar media in a variety of electrochemical systems [18,19]. They are room temperature molten salts that typically consist of bulky, asymmetric organic cations and inorganic anions, and possess many attractive properties such as non-volatility, non-flammability, excellent thermal stability, high ionic conductivity, and wider electrochemical windows [18–23]. More recently, ionic-liquid-based polymer gel electrolytes have also been examined for application as promising electrolytes in batteries, supercapacitors and fuel cells [18,19,24–28].

In this work, we report a novel magnesium ion conducting, gel polymer electrolyte system based on a room temperature ionic liquid that consists of 1-ethyl-3-methylimidazolium trifluoromethanesulfonate (EMI triflate), abbreviated as EMITf and its solution with magnesium trifluoromethanesulfonate, i.e., magnesium triflate or $Mg(Tf)_2$ immobilized in the polymer matrix, poly(vinylidenefluoride-co-hexafluoropropylene) (PVdF-HFP). A wide variety of experiments, namely, X-ray diffraction, thermal analysis, infrared spectroscopy, complex impedance analysis, conductivity versus $1/T$ and composition, transference number and cyclic voltammetry have been carried out to characterize the gel polymer electrolyte and to establish ion transport behaviour in the material. It has been observed that the PVdF-HFP/ionic liquid/Mg-salt gel system under study is a Mg^{2+} ion conductor together with a substantial contribution to the total conductivity due to the anions. Although, a contribution to the total ionic transport due to the component ions of ionic liquids cannot be ruled out.

2. Experimental

1-Ethyl-3-methylimidazolium trifluoromethanesulfonate (EMITf), poly(vinylidenefluoride-hexafluoropropylene) (PVdF-HFP) and magnesium trifluoromethanesulfonate $Mg(Tf)_2$ were purchased from Sigma–Aldrich and used as-received. A solution-cast method was used to produce polymer gel electrolyte films. First, the liquid electrolyte was prepared by dissolving 0.3 M magnesium salt in ionic liquid. The polymer PVdF-HFP was separately dissolved in acetone. The liquid electrolyte was then mixed with the PVdF-HFP/acetone solution and stirred magnetically for 4–5 h. The weight ratio of the liquid electrolyte to PVdF-HFP was controlled at 4:1. The viscous mixture was cast over glass petri dishes and acetone was allowed to evaporate slowly. Finally, free-standing polymer gel electrolyte films (thickness ~400–450 μm), as typically shown in Fig. 1, were obtained. Gel polymer electrolyte films comprised of EMITf and PVdF-HFP in different weight ratios were also prepared for comparison following the same procedure mentioned above.

The thermal stabilities of polymer gel electrolytes were measured by thermo-gravimetric analysis (TGA) and differential scanning calorimetry (DSC). The TGA was carried out from room temperature to 250 °C under a dynamic dry nitrogen atmosphere at a heating rate of 10 °C min^{-1} using a PerkinElmer TGA7 instrument. The DSC was performed with a TA Instruments, Model: Q100 system. Measurements were carried out from −90 to 250 °C at a heating rate of 10 °C min^{-1} in a static nitrogen atmosphere. The

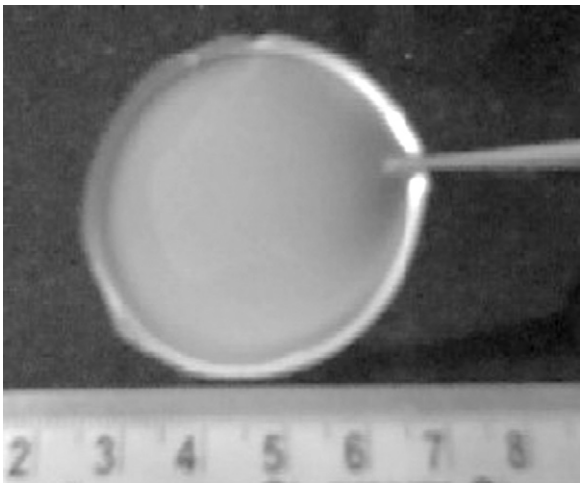

Fig. 1. Photograph of $Mg(Tf)_2$/EMITf/PVdF-HFP polymer gel electrolyte film.

morphology of the gel polymer electrolyte films was observed using a scanning electron microscope (JEOL JSM 5600). The measurements were performed under a low vacuum after sputtering the samples with gold to prepare a conductive surface. X-ray diffraction patterns of the films were recorded by means of a Philips X-ray diffractometer with Cu Kα radiation over the Bragg angle (2θ) range of 5–60°. Fourier transform infra-red (FTIR) spectra were taken with a PerkinElmer FTIR spectrophotometer.

The electrical conductivity of the ionic liquid EMITf and $Mg(Tf)_2$/EMITf liquid electrolyte and gel polymer electrolyte films was evaluated by means of an AC impedance technique using a LCR Hi-Tester (HIOKI-3522-50, Japan) over the frequency range 100 kHz to 1 Hz with a signal level of 10 mV. The conductivity of the ionic liquid and the liquid electrolyte was evaluated using a special two-electrode conductivity cell. Conductivity measurements of gel polymer films were performed by sandwiching the films between two stainless-steel foils. Cyclic voltammograms of the symmetric cells, SS/GPE/SS (SS: stainless steel) and Mg/GPE/Mg, were recorded with a CHI 608C Electrochemical Analyzer at a scan rate of 5 mV s^{-1}. The electrochemical stability of the electrolyte films was evaluated by means of linear sweep voltammetry using stainless steel as the working electrode and a Mg disc as both the counter and the reference electrode.

The total ionic transport number (t_{ion}) was evaluated by the polarization technique [29]. In this technique, the SS/electrolyte/SS cell was polarized by applying a step potential (1.0 V) and the resulting potentiostatic current was monitored as a function of time. The stainless steel (SS) acted as blocking electrodes. The value of t_{ion} was determined using the formula:

$$t_{ion} = \frac{i_T - i_e}{i_T} \quad (1)$$

where i_T and i_e are the total and the residual current, respectively. The transport number (t_+) of Mg^{2+} ions in the GPE was evaluated by the method of Evans et al. [30] using the combination of AC impedance spectroscopy and DC polarization of a Mg/electrolyte/Mg cell.

3. Results and discussion

3.1. Structural studies

XRD patterns of the PVdF-HFP film recast from its acetone solution, the EMITf/PVdF-HFP blend film and the $Mg(Tf)_2$/EMITf/PVdF-

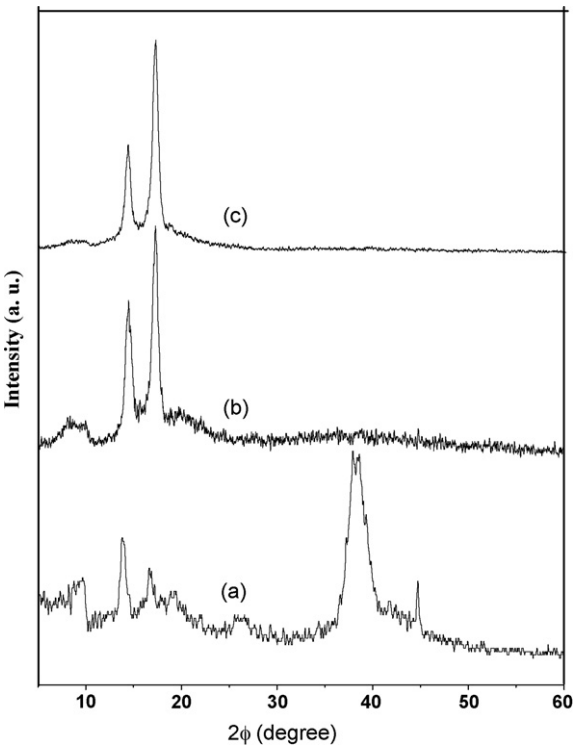

Fig. 2. XRD patterns of: (a) PVdF-HFP film, (b) EMITf/PVdF-HFP blend, and (c) $Mg(Tf)_2$/EMITf/PVdF-HFP polymer gel electrolyte film.

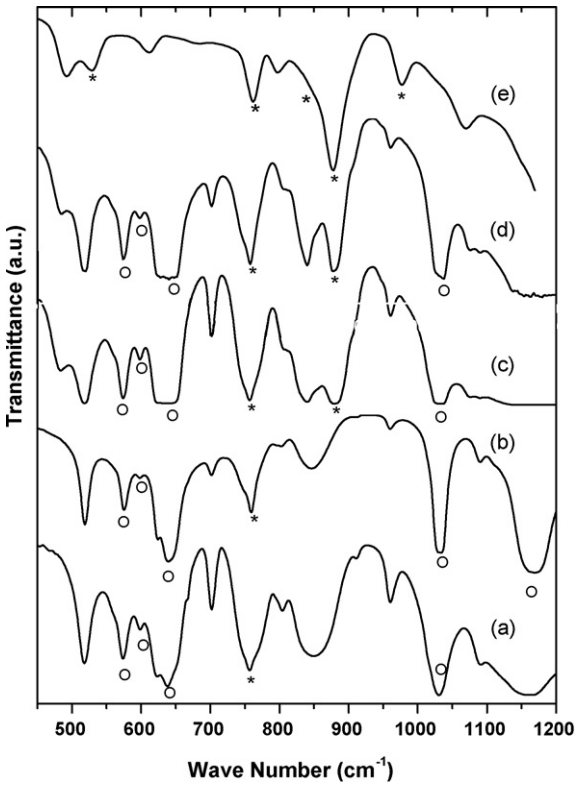

Fig. 3. FTIR spectra of: (a) ionic liquid EMITf, (b) EMITf/$Mg(Tf)_2$ solution, (c) EMITf/PVdF-HFP blend film, (d) $Mg(Tf)_2$/EMITf/PVdF-HFP gel polymer electrolyte, and (e) PVdF-HFP (pure) film.

HFP gel polymer electrolyte film are shown in Fig. 2. The XRD pattern of the PVdF-HFP film shows the typical characteristic of a semi-crystalline microstructure, i.e., the co-existence of mixed crystalline and amorphous regions with predominant peaks at $2\theta = 14.6^\circ$, 17°, 20°, 26.6° and 38° (Fig. 2a). After blending with the ionic liquid or the Mg-salt/ionic liquid solution, some of the peaks of PVdF-HFP ($\sim 27^\circ$, 38° and 49°) disappear. This indicates that the ionic liquid or the Mg-salt/ionic liquid solution most likely blends with the PVdF-HFP at the molecular level and functions as a plasticizer for the polymer. The crystalline nature of the host polymer PVdF-HFP still persists as evident from the observation of more distinct and predominant peaks at 14.6 and 17°.

FTIR spectroscopic studies were conducted to investigate the ion and ionic liquid interaction with the host polymer, PVdF-HFP in the gel electrolyte system at the microscopic level and possible conformational changes in the host polymer due to Mg-salt/ionic liquid entrapment. Fig. 3 shows the comparative FTIR spectra of the ionic liquid EMITf, $Mg(Tf)_2$/EMITf solution, EMITf/PVdF-HFP blend film, $Mg(Tf)_2$/EMITf/PVdF-HFP gel polymer electrolyte film and pure polymer PVdF-HFP in the wave number region of 450–1200 cm^{-1}. The following distinctive features can be extracted from the spectral response:

(i) The conformational changes in the semi-crystalline host polymer PVdF-HFP due to the addition of ionic liquid or ionic liquid/Mg-salt solution have been monitored. The peaks corresponding to the bands at 530, 762, 840 (very weak), 878 and 976 cm^{-1} (marked by stars in Fig. 3e) are observed and assigned in Table 1. In particular, the intense peaks at 530 and 976 cm^{-1} are due to $TGTG^-$ (T: trans and G: gauche) conformation (i.e., α-phase) of the semi-crystalline PVdF-HFP [31,32]. Other bands are either very weak or overlapping with the bands associated with the ionic liquid or Mg-salt. Two peaks (878 and 976 cm^{-1}) have been examined more closely to see the changes, as shown in the expanded curves in the range 800–1000 cm^{-1} (Fig. 4A). A comparison indicates that the band at 976 cm^{-1} (assigned to the α-phase) disappears due to the addition of ionic liquid or ionic liquid/Mg-salt solution (Fig. 4A, c–e). It may be noted that the band at 530 cm^{-1}, assigned to α-phase of PVdF-HFP, has also disappeared (Fig. 3). Further, the band at 878 cm^{-1} (assigned to the amorphous phase), which appears as a symmetrical peak, becomes appreciably broad and appears to be the sum of two peaks (Fig. 4A, c–e). These observations indicate the occurrence of substantial conformational changes in the crystalline texture of the host polymer PVdF-HFP due to interaction with the ionic liquid/Mg-salt in the gel polymer electrolyte. In particular, the disappearance of bands associated with the crystalline α-phase and broadening of the band of the amorphous phase of the polymer indicate a reduction in crystallinity and the dominance of the amorphous phase in the gel polymer electrolyte.

Table 1
Assignment of important FTIR bands of PVdF-HFP and triflate anion $(CF_3SO_3)^-$.

	IR bands (cm^{-1})	Assignment
PVdF-HFP	530	α-Phase
	762	
	840 (very weak)	
	976	
	878	Amorphous phase
$(CF_3SO_3)^-$	574	$\delta_a(CF_3)$
	596	Ion pairs/aggregates
	640	$\delta_a(SO_3)$
	756	$\delta_s(CF_3)$
	1032	$\nu_s(SO_3)$
	1157	$\nu_a(SO_3)$

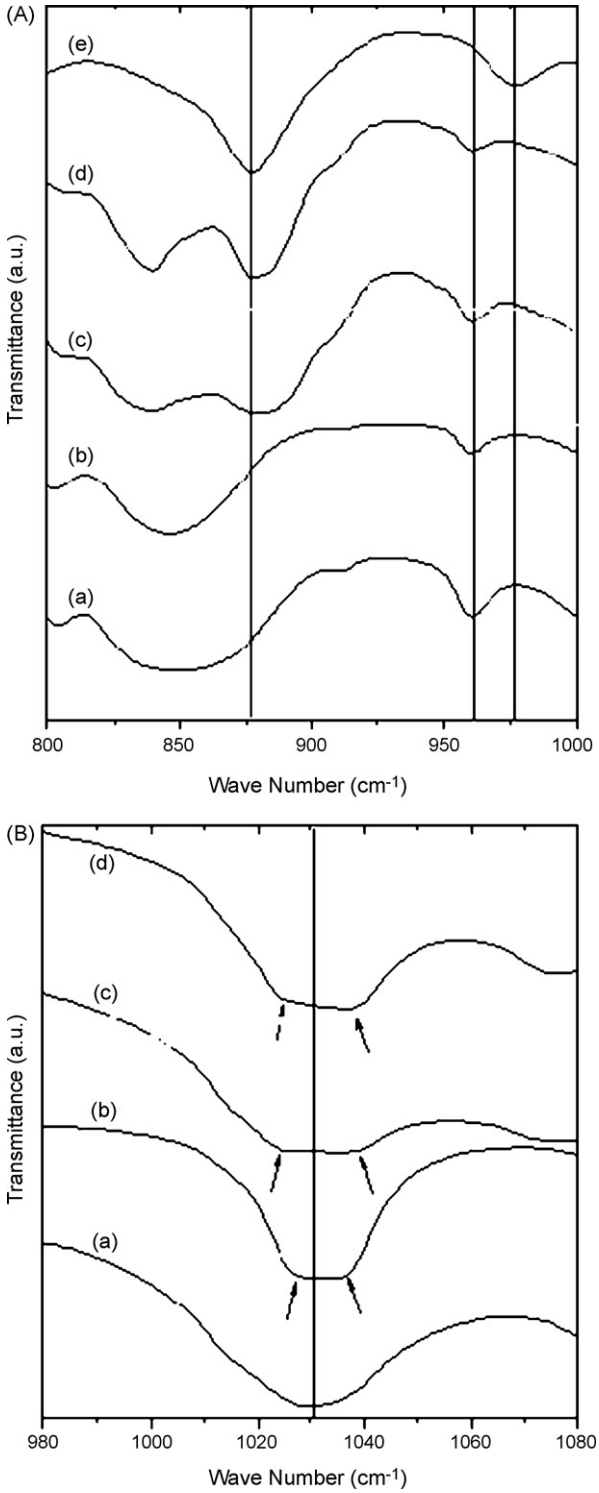

Fig. 4. Expanded representation of FTIR spectra: (A) for ionic liquid EMITf (a), EMITf/$Mg(Tf)_2$ solution (b), EMITf/PVdF-HFP blend (c), $Mg(Tf)_2$/EMITf/PVdF-HFP gel electrolyte (d), PVdF-HFP (pure) film (e) in 800–1000 cm^{-1} region; (B) for ionic liquid EMITf (a), EMITf/$Mg(Tf)_2$ solution (b), EMITf/PVdF-HFP blend (c), $Mg(Tf)_2$/EMITf/PVdF-HFP gel electrolyte (d) in 980–1080 cm^{-1} region.

(ii) The possible effects on the ionic liquid and Mg-salt solution in the ionic liquid due to entrapment in polymer host have also been examined. Bands associated with the triflate-anion $(CF_3SO_3)^-$ are observed at 574, 596, 640, 756, 1032 and 1157 cm^{-1}; these are assigned in Table 1. The bands are indicated by open circles in the spectra (Fig. 3). The peaks located at 574, 640 and 756 cm^{-1} are attributed to free triflate anions [33–36], whereas that at 596 cm^{-1} is sensitive to ion pair/aggregate formation [37]. Significant changes (i.e., shifting, broadening, etc.) in these peaks are not observed in the gel polymer film compared with the ionic liquid or ionic liquid/Mg-salt solution. On the other hand, a significant change in the peak texture is found in the band at 1032 cm^{-1}, which is assigned to $\nu_s(SO_3)$-symmetric stretching of SO_3 [Table 1]. An expanded portion of the spectra around 1032 cm^{-1} is shown in Fig. 4B. The band at 1032 cm^{-1} associated with the triflate ion of pure EMITf [$\nu_s(SO_3)$] appears to be almost symmetrical [Fig. 4B(a)]. On addition of $MgTf_2$, however, the texture of the peak changes and appears to be the sum of two nearby peaks [Fig. 4B(b)]. This may be attributed to $\nu_s(SO_3)$ modes associated with the co-existence of free triflate anions and ion pairing with Mg^{2+} and/or EMI^+ cations. When the EMITf or EMITf/$MgTf_2$ solution is trapped in the host polymer PVdF-HFP, the peak becomes broader as if the two peaks disperse more and become well separated. This indicates anion–polymer interaction in the EMITf/PVdF-HFP blend $Mg(Tf)_2$/EMITf/PVdF-HFP gel polymer electrolyte.

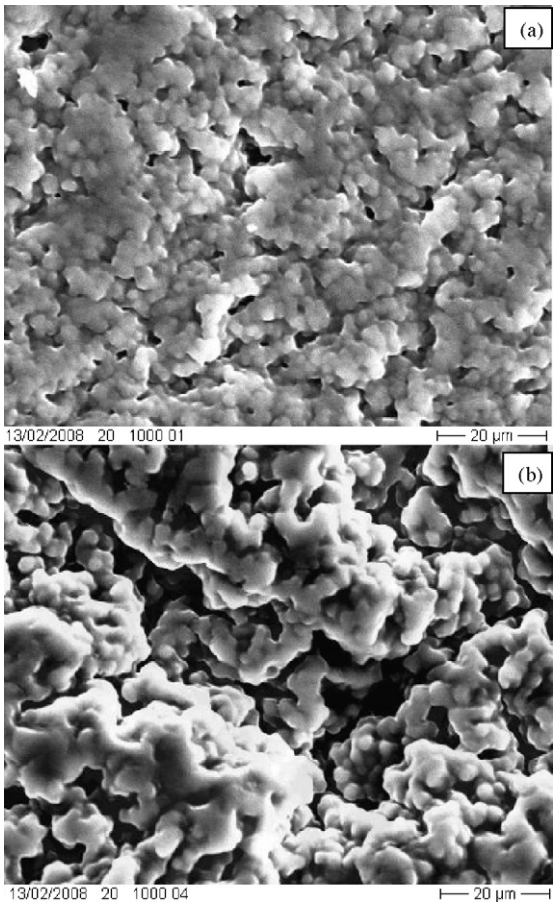

Fig. 5. SEM images of: (a) EMITf/PVdF-HFP blend; (b) $Mg(Tf)_2$/EMITf/PVdF-HFP gel polymer electrolyte film.

The morphology of the EMITf/PVdF-HFP blend film and $Mg(Tf)_2$/EMITf/PVdF-HFP gel polymer electrolyte film has been examined by SEM and images are presented in Fig. 5. The EMITf/PVdF-HFP blend film is seen to have a uniformly small pore size at the microscopic level (Fig. 5a). Slightly larger, but uniformly distributed pores are also observed in the Mg-salt/ionic liquid/PVdF-HFP gel polymer electrolyte film (Fig. 5b). The uni-

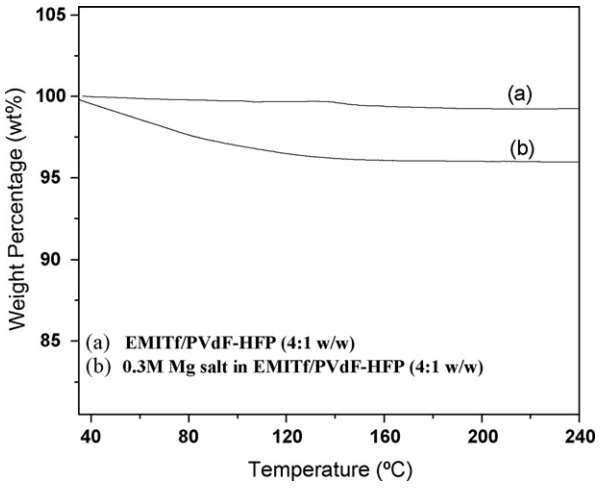

Fig. 6. TGA of: (a) EMITf/PVdF-HFP blend; (b) $Mg(Tf)_2$/EMITf/PVdF-HFP gel electrolyte film.

formly dispersed pores in the polymer microstructure lead to the retention of ionic liquid or liquid electrolyte and thereby better connectivity through the polymer that gives rise to high ionic conductivity.

3.2. Thermal studies

Fig. 6 shows TGA results for the EMITf/PVdF-HFP blend film and the $Mg(Tf)_2$/EMITf/PVdF-HFP gel polymer electrolyte film. Almost no loss in weight is observed for the ionic liquid/polymer blend up to 250 °C. This indicates that no component is volatile in the blend film. A slight weight loss (up to the maximum of ~4 wt.%) is found in the case of the $Mg(Tf)_2$/EMITf/PVdF-HFP gel polymer electrolyte film, gradually up to ~100 °C. This is most likely due to moisture absorption in the film given that the Mg-salts are quite sensitive to moisture. Thereafter, no further weight loss is recorded up to 250 °C. The non-volatility is of special importance for the potential application of the gel polymer films as electrolyte/separator components in Mg batteries.

DSC curves of the PVdF-HFP film, the EMITf/PVdF-HFP blend film and the Mg-salt/EMITf/PVdF-HFP gel polymer electrolyte film are presented in Fig. 7(a–c). The endothermic peak at 140 °C corresponds to the melting of the polymer PVdF-HFP film. Blending with a ionic liquid or a liquid electrolyte Mg-salt/EMITf lowers the melting point to 109 °C. The melting peaks become more asymmetric and broad and this is attributed to the presence of liquid components that cause an increase in the amorphous proportion in the overall material. The endothermic peak around −20 °C observed in both the EMITf/PVdF-HFP blend and the Mg-salt/EMITf/PVdF-HFP electrolyte is due to melting of the ionic liquid, EMITf [17]. The electrolyte film remains stable in the gel phase over a substantially wide temperature range from −30 to 110 °C, which is advantageous for their potential applications in electrochemical devices.

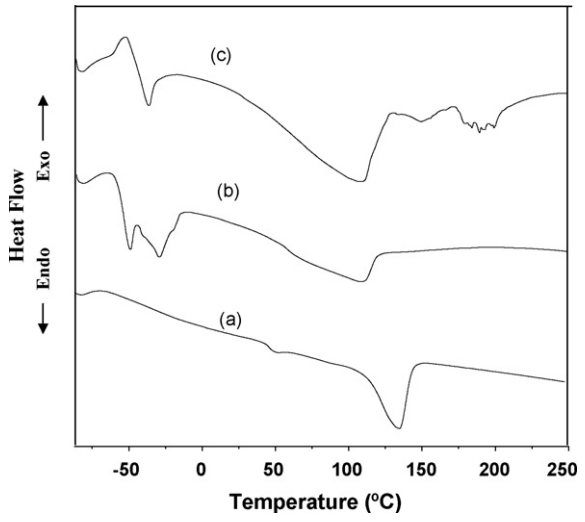

Fig. 7. DSC curves of: (a) PVdF-HFP (pure) film; (b) EMITf/PVdF-HFP blend; (c) $Mg(Tf)_2$/EMITf/PVdF-HFP gel electrolyte film.

Table 2
Electrical conductivity of ionic liquid, Mg-salt/ionic liquid solution and gel polymer electrolyte film.

Material	σ (S cm^{-1}) at room temperature (~20 °C)
EMITf	6.4×10^{-3}
0.3M $Mg(Tf)_2$ in EMITf	4.8×10^{-3}
EMITf/PVdF-HFP (1:1, w/w)	2.3×10^{-4}
EMITf/PVdF-HFP (2.33:1, w/w)	5.1×10^{-3}
EMITf/PVdF-HFP (4:1, w/w)	6.3×10^{-3}
0.3M $Mg(Tf)_2$ in EMITf/PVdF-HFP (4:1, w/w)	3.4×10^{-3}

3.3. Electrical and electrochemical properties

Table 2 lists the electrical conductivity of the ionic liquid, the Mg-salt/ionic liquid solution and the polymer gel electrolyte films. The ionic liquid EMITf exhibits an electrical conductivity of ~6.4×10^{-3} S cm^{-1} at 20 °C. A slight decrease in the conductivity has been observed due to the addition of the Mg-salt in ionic liquid. This is attributed to the possible increase in viscosity of the ionic liquid when Mg-salt is added. Such an increase in viscosity, and hence decrease in conductivity, has been reported for lithium salt/ionic liquid mixtures [38,39]. While preparing the gel polymer electrolytes, the composition of the blend of polymer, PVdF-HFP and ionic liquid, EMITf was optimized first from the electrical conductivity and mechanical/dimensional stability points of view. A 1:1 (w/w) ionic liquid/polymer composition offers a relatively lower conductivity (Table 2) with substantially higher mechanical strength which is, of course, due to the higher content of polymer. The conductivity increases substantially (~20 times) when the ionic liquid/polymer ratio is 2.33:1 (w/w) (Table 2). On decreasing the polymer content further, the blend offers substantially good conductivity at a ratio of 4:1 w/w ionic liquid/polymer system, which is obtained in the form of a free-standing film with appreciable mechanical/dimensional stability. Further, the room temperature electrical conductivity of the blend with a ratio of 4:1 (w/w) ionic liquid/polymer ratio has a value comparable with that of the pure ionic liquid EMITf (Table 2), and hence it is chosen for gel electrolyte preparation with the Mg-salt. On addition of $Mg(Tf)_2$ to EMITf/PVdF-HFP, a decrease in conductivity is observed in the gel electrolyte film (Table 2). This suggests that blending of the liquid electrolyte ($Mg(Tf)_2$/EMITF system) with the, PVdF-HFP polymer occurs at the molecular level. The ionic conductivity would not be decreased to such an extent if the blending were at the microscopic level rather than the molecular level [40,41].

The temperature dependence of the ionic liquid EMITf, the liquid electrolyte (ionic liquid/Mg-salt), the EMITf/PVdF-HFP blend film and the $Mg(Tf)_2$/EMITf/PVdF-HFP gel polymer electrolyte film is presented in Fig. 8. A lowering of the conductivity due to the addition of Mg-salt in the ionic liquid is found at all temperatures with almost same slope of variation (Fig. 8a). This further confirms the influence of the viscosity of the liquid electrolyte, as discussed above. The temperature dependence of the ionic liquid and liquid

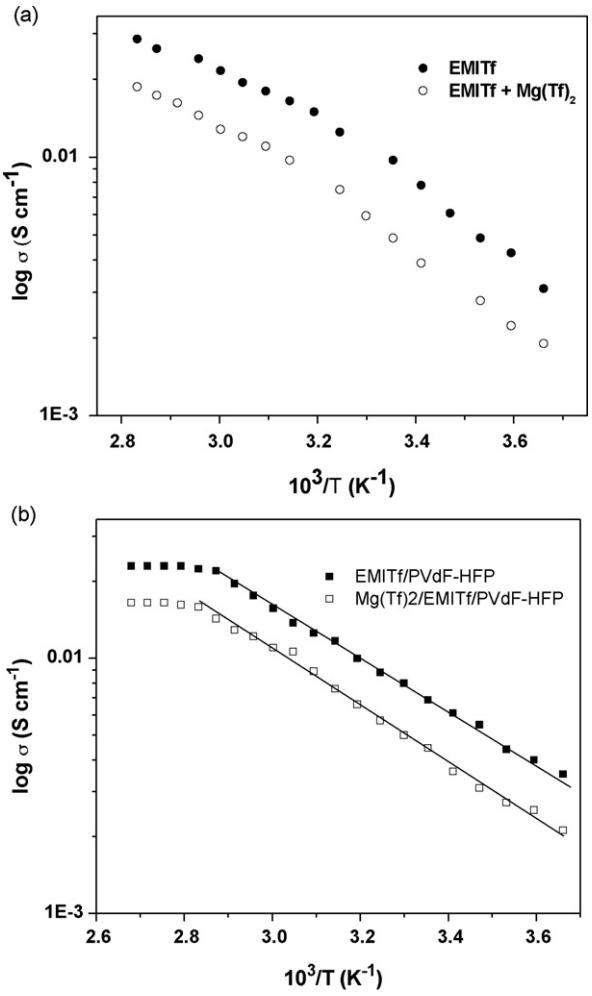

Fig. 8. σ vs. $1/T$ plots of: (a) pure ionic liquid EMITf and 0.3 M $Mg(Tf)_2$ solution in EMITf; (b) EMITf/PVdF-HFP blend and $Mg(Tf)_2$/EMITf/PVdF-HFP gel polymer electrolyte film.

electrolyte shows non-Arrhenius Vogel–Tammen–Fulcher (VTF) behaviour as expressed by the following equation:

$$\sigma = AT^{-1/2} \exp\left(\frac{-B}{T - T_0}\right) \quad (2)$$

where the parameter B is associated with rate at which viscosity changes with temperature, A is a constant (pre-exponential factor, i.e., the conductivity at infinitely high temperature), and T_0 is close to the glass transition temperature. These fitting parameters

Table 3
(a) Different parameters (A, B, and T_0) for ionic liquid, ionic liquid–Mg-salt solution obtained by fitting of conductivity to VTF equation; (b) different parameter (σ_0 and E_a) for ionic liquid/polymer blend and Mg-salt/ionic liquid/polymer gel polymer electrolyte obtained by linear fitting of conductivity to Arrhenius equation.

Materials	Parameters		
	A (S cm^{-1} K$^{1/2}$)	B (eV)	T_0 (K)
(a)			
EMITf	0.546	0.23	248
$Mg(Tf)_2$/EMITf solution	0.745	0.24	261
Materials		σ_0 (S cm^{-1})	E_a (eV)
(b)			
EMITf/PVdF-HFP blend		6.3×10^{-2}	0.201
$Mg(Tf)_2$/EMITf/PVdF-HFP gel electrolyte		1.03×10^{-2}	0.216

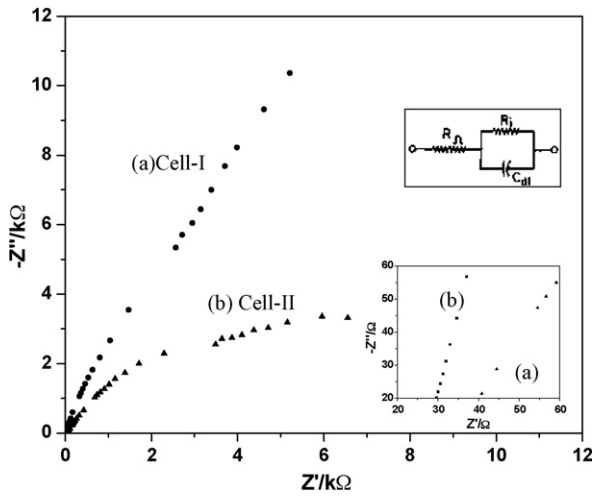

Fig. 9. Complex impedance plots for: (a) Cell-I: SS | gel electrolyte | SS; (b) cell-II: Mg | gel electrolyte | Mg recorded at room temperature. High frequency region expanded and shown in inset. Bulk resistance of polymer gel electrolyte (R_Ω) and interfacial resistance (R_i) evaluated using an equivalent circuit shown in inset.

have been evaluated and are listed in Table 3a. The temperature dependence of the conductivity of the EMITf/PVdF-HFP blend shows a similar trend to that of the $Mg(Tf)_2$/EMITf/PVdF-HFP gel polymer electrolyte (Fig. 8b). This suggests that these films likely retain the same ionic conduction mechanism in the temperature range from 0 to 80 °C, which is consistent with their single-phase nature as revealed by DSC. For the polymer gel electrolyte containing the higher content of liquid electrolyte, EMITf functions as both a plasticizer for the polymer matrix and a solvation medium for the electrolyte salt. The polymer PVdF-HFP provides mechanical support and dimensional stabilization through polymer chain entanglements and/or chemical cross-linking. The 'σ versus $1/T$' curves for both the ionic liquid/polymer blend and the gel polymer electrolyte show a linear pattern up to ~80 °C, thereafter no conductivity enhancement is observed (Fig. 8b). The linear pattern is suggestive of an Arrhenius-type, thermally activated process following the expression:

$$\sigma = \sigma_0 \exp\left(\frac{-E_a}{kT}\right) \quad (3)$$

where E_a is the activation energy, σ_0 is a pre-exponential factor and k is the Boltzmann constant. These parameters have been evaluated and listed in Table 3b. The Mg^{2+} conducting polymer gel electrolyte has an ionic conductivity of the order of $\sim 1 \times 10^{-3}$ S cm^{-1} at 0 °C and 2×10^{-2} S cm^{-1} at 80 °C. Thus, it shows promise for application in Mg batteries over a wide temperature range.

In order to confirm Mg^{2+} conduction in the gel polymer electrolyte film, complex impedance spectroscopy and cyclic voltammetric studies have been carried out on the symmetrical SS/gel electrolyte/SS (Cell-I) and Mg/gel electrolyte/Mg (Cell-II) cells. In Cell-I, the gel film is in contact with the stainless steel (SS, a blocking electrode), whereas Mg foil is used as reversible electrodes in Cell-II. Comparative impedance complex plots for Cell-I and Cell-II recorded at room temperature (~20 °C) are given in Fig. 9. The SS foil serves as the current collector in Cell-II. The impedance response of Cell-I (with SS electrodes) shows the uprising behaviour of imaginary impedance at the lower frequency range; this indicates the blocking nature of the SS electrodes (Fig. 9a). On the other hand, an almost well-defined semicircular dispersion curve is observed in the case of Cell-II (with Mg electrodes, Fig. 9b). This behaviour is similar to that reported for a Li/gel electrolyte/Li cell [42] and clearly suggests that the Mg metal attains equilibrium

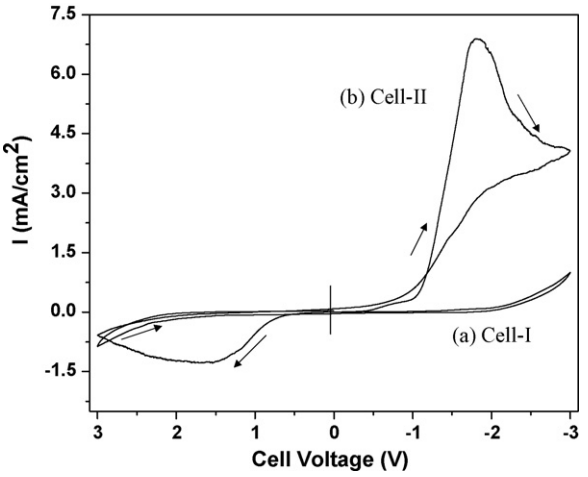

Fig. 10. Cyclic voltammograms of: (a) cell-I: SS | gel electrolyte | SS; (b) cell-II: Mg | gel electrolyte | Mg; recorded at room temperature at scan rate of 5 mV s^{-1}.

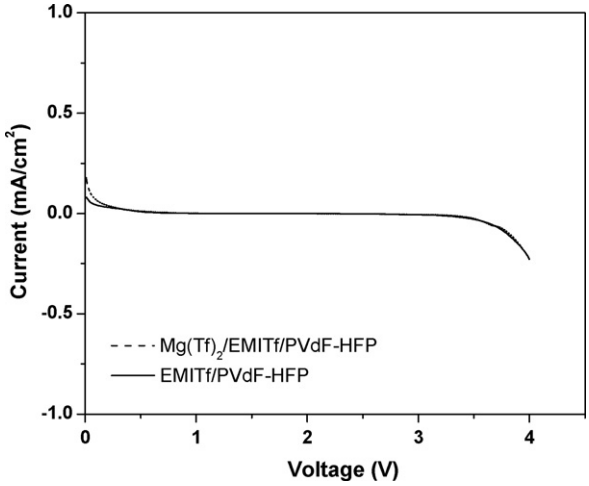

Fig. 11. Linear sweep voltammograms of EMITf/PVdF-HFP and $Mg(Tf)_2$/EMITf/PVdF-HFP gel electrolyte films using SS/electrolyte/Mg cells at scan rate of 5 mV s^{-1}.

with the Mg^{2+} ions in the gel polymer electrolyte. A possible electrical equivalent circuit is shown in the inset of Fig. 9. The bulk resistance of the gel film (R_Ω) has been obtained from the high-frequency intercept of the complex plane plots and the interfacial resistance (R_i) has been calculated from the low-frequency intercept. The values of R_Ω measured for both cells are almost in the same range (~30–40 Ω cm^2). The value of R_i for the Mg/gel electrolyte is ~6 kΩ cm^2, whereas that for the SS/GPE is ~80 kΩ cm^2. The substantially lower value of R_i for the Mg/GPE interface further confirms that equilibrium has been established between Mg metal and Mg^{2+} ions and that Mg^{2+} conduction takes place in the gel polymer electrolyte.

Cyclic voltammetric study on these two cells further confirms the Mg^{2+} conduction in the gel polymer electrolyte film, as described as follows. The cyclic voltammograms for the two cells at a scan rate of 5 mV s^{-1} is shown in Fig. 10. The cathodic and anodic current peaks are distinctly observed for the cell-II (with Mg electrodes), whereas no such features are evident in the case of Cell-I (with SS electrodes) in the same potential range (Fig. 10). Further, the magnitude of the currents in Cell-II is several times higher than for Cell-I. This suggests that the cathodic deposition and anodic oxidation of Mg are facile at the Mg/gel electrolyte interface and hence are indicative of Mg^{2+} conduction in the gel polymer electrolyte film. It may be noted that the cathodic/anodic peak potentials are separated by several volts, similar to other systems, e.g., the Li/PEO + $LiBF_4$ film/Li cell as reported by Munichandraiah et al. [43]. This is possible because the experiments were carried out with the symmetrical cell with a two-electrode geometry without using a reference electrode.

The electrochemical stability of the gel polymer electrolyte film has also been tested using linear sweep voltammetry (LSV) recorded on the SS/gel electrolyte/Mg cell. As observed in Fig. 11, the electrolyte films are stable up to ~3.5 V. This value of the working voltage range (i.e., electrochemical potential window) appears to be sufficiently high to use the gel polymer electrolyte film as solid-state like separator/electrolyte in Mg-batteries and supercapacitors.

The total ionic (cationic and anionic) transport number (t_{ion}) has been evaluated using Wagner's polarization method, as described in Section 2. The value of t_{ion} is determined from using Eq. (1) and found to be >0.99. This shows that the total conductivity is predominantly ionic. No electronic conductivity is expected in the gel-like electrolytes where liquid electrolytes are trapped in the almost inert network of polymer hosts and liquid-like charge transport takes place in such systems. Further, different ionic species are expected to be mobile in gel polymer electrolytes in which ionic liquids are used as liquid electrolyte [44]. Only the target ion alone (e.g., Mg^{2+} in the present case) would not be transported, rather component ions of ionic liquid would also migrate on application of an electric field. Three types of ions (two cations viz., Mg^{2+} and EMI^+ and one anion, $CF_3SO_3^-$, common to both the salt and ionic liquid used) are expected to be mobile in the present gel system. An effort has been made to evaluate the transport number (t_+) of Mg^{2+} ions in the gel polymer electrolyte using a combination of AC and DC techniques, as proposed by Evans et al. [30]. In this technique, a Mg/gel electrolyte/Mg cell was polarized potentiostatically by applying a voltage of $\Delta V = 0.5$ V for 4–5 h and initial and final currents were recorded. As a part of the technique, the cell was subjected to AC impedance measurements both prior to and after the polarization and the values of the electrode-electrolyte contact resistances were obtained. The value of t_+ can be obtained from:

$$t_+ = \frac{I_s(\Delta V - R_0 I_0)}{I_0(\Delta V - R_s I_s)} \quad (4)$$

where I_0 and I_s are the initial and final steady-state currents and R_0 and R_s are the cell resistances before and after the polarization, respectively. The value of t_+ so obtained for the $Mg(Tf)_2$/EMITf/PVdF-HFP gel polymer electrolyte is ~0.26 at room temperature. This value for the Mg^{2+} ion suggests a substantial contribution of anions and ionic liquid components to the total ionic conduction in the electrolyte. Efforts are continuing to overcome such problems by choosing various ionic liquids and salts of different anions in gel polymer systems.

4. Conclusions

A novel magnesium ion conducting gel polymer electrolyte consisting of a liquid electrolyte solution of $Mg(Tf)_2$ salt in an ionic liquid, EMITf, immobilized in a host polymer PVdF-HFP has been synthesized and characterized. A blend of PVdF-HFP and ionic liquid has also been prepared for comparison. On the basis of various structural, thermal, electrical and electrochemical studies, the following conclusions have been drawn:

(i) The polymer gel electrolyte film is flexible and free-standing with good mechanical strength.

(ii) The film offers high ionic conductivity ($\sigma \sim 10^{-3}$ S cm^{-1} at room temperature) with a wider electrochemical potential window and excellent thermal stability having single-phase behaviour for a temperature range from −30 to 110 °C.
(iii) There are substantial conformational changes in the crystalline texture of the host polymer PVdF-HFP due to immobilization of the ionic liquid/Mg-salt in the gel polymer electrolyte. The existence of free anions and ion (particularly triflate anion)–polymer interaction has also been detected from the FTIR studies.
(iv) Studies based on AC impedance spectroscopy and cyclic voltammetry indicate the existence of an electrochemical equilibrium between Mg metal and Mg^{2+} ions and hence confirm Mg^{2+} ion conduction in the polymer gel electrolyte.
(v) The Mg^{2+} ion transport number is ∼0.26, which indicates a lower contribution to the overall ionic conductivity. The other possible mobile ions are ionic liquid components and triflate anions, which are common to both the ionic liquid and magnesium salt in the present studies.
(vi) The present ionic-liquid-based polymer gel electrolyte appears to be an excellent substitute for the liquid electrolyte in electrochemical devices, particularly in rechargeable magnesium batteries.

Acknowledgements

Authors acknowledge the financial support received from University of Delhi (under the Scheme to strengthen R&D Doctoral Research Programme providing funds to University faculty, 11-17 Research Fund, 2007) and the Council of Scientific & Industrial Research, New Delhi (Sanction No.: 03(1069)/06/EMR-II, 2006).

References

[1] J.-M. Tarascon, M. Armand, Nature 414 (2001) 359–367.
[2] P. Novak, W. Scheifele, O. Hass, J. Power Sources 54 (1995) 479–482.
[3] D. Aurbach, Y. Gofer, Z. Lu, A. Schechter, O. Chusid, H. Gizbar, Y. Cohen, V. Ashkenazi, M. Moshkovich, R. Turgeman, E. Levi, J. Power Sources 97–98 (2001) 28–32.
[4] J.L. Robinson, in: N.C. Cohoon, G.W. Heise (Eds.), The Primary Battery, vol. II, Wiley, New York, 1976, p. p.149.
[5] D. Aurbach, Z. Lu, A. Schechter, Y. Gofer, H. Gizbar, R. Turgeman, Y. Cohen, M. Moshkovich, E. Levi, Nature 407 (2000) 724–727.
[6] D. Aurbach, I. Weissman, Y. Gofer, E. Levi, Chem. Rec. 3 (2003) 61–73.
[7] E. Lancry, E. Levi, Y. Gofer, M. Levi, G. Salitra, D. Aurbach, Chem. Mater. 16 (2004) 2832–2838.
[8] Z. Lu, A. Schechter, M. Moshlovich, D. Aurbach, J. Electroanal. Chem. 466 (1999) 203–217.
[9] A. Manuel Stephan, Eur. Polym. J. 42 (2006) 21–42.
[10] S.A. Hashmi, Natl. Acad. Sci. Lett. 27 (2004) 27–46.
[11] N. Yoshimoto, S. Yakushiji, M. Ishikawa, M. Morita, Solid State Ionics 152–153 (2002) 259–266.
[12] G.G. Kumar, N. Munichandraiah, Electrochim. Acta 47 (2002) 1013–1022.
[13] D.K. Rai, S.A. Hashmi, Y. Kumar, G.P. Pandey, in: S.A. Hashmi, Amita Chandra, Amreesh Chandra (Eds.), Electroactive Polymers: Materials and Devices, vol. II, Allied Publishers, New Delhi, 2007, pp. 407–411.
[14] C. Liebenow, Solid State Ionics 136–137 (2000) 1211–1214.
[15] G.G. Kumar, N. Munichandraiah, J. Power Sources 91 (2000) 157–160.
[16] M. Morita, N. Yoshimoto, S. Yakushiji, M. Ishikawa, Electrochem. Solid-State Lett. 4 (2001) A177–A179.
[17] F.B. Dias, L. Plomp, J.B.J. Veldhuis, J. Power Sources 88 (2000) 169–191.
[18] Christopher S. Brazel, Robin D. Rogers (Eds.), Ionic Liquids in Polymer Systems, ACS Symposium Series 913, American Chemical Society, Washington, DC, 2005.
[19] H. Ohno (Ed.), Electrochemical Aspects of Ionic Liquids, Wiley Interscience, New Jersey, 2005.
[20] P. Bonhote, A.-P. Dias, N. Papageorgiou, K. Kalyanasundaram, M. Gratzel, Inorg. Chem. 35 (1996) 1168–1178.
[21] A. Webber, G.E. Blomgrem, in: W.A.V. Schalkwijk, B. Scrosati (Eds.), Advances in Lithium-Ion Batteries, Kluwer Academic/Plenum, New York, 2002, pp. 185–232.
[22] M. Galinski, A. Lewandowski, I. Stepniak, Electrochim. Acta 51 (2006) 5567–5580.
[23] D.R. Macfarlane, M. Forsyth, P.C. Howlett, J.M. Pringle, J. Sun, G. Annat, W. Neil, E.I. Izgorodina, Acc. Chem. Res. 40 (2007) 1165–1173.
[24] M. Morita, T. Shirai, N. Yoshimoto, M. Ishikawa, J. Power Sources 139 (2005) 351–355.
[25] K.-S. Kim, S.-Y. Park, S. Choi, H. Lee, J. Power Sources 155 (2006) 385–390.
[26] Hui Ye, J. Huang, J.J. Xu, A. Khalfan, S.G. Greenbaum, J. Electrochem. Soc. 154 (2007) A1048–A1057.
[27] W. Lu, K. Henry, C. Turchi, J. Pellegrino, J. Electrochem. Soc. 155 (2008) A361–A367.
[28] S.S. Sekhon, B.S. Lalia, J.-S. Park, C.-S. Kim, K. Yamada, J. Mater. Chem. 16 (2006) 2256–2265.
[29] S.A. Hashmi, S. Chandra, J. Mater. Sci. Eng. B 34 (1995) 18–26.
[30] J. Evans, C.A. Vincent, P.G. Bruce, Polymer 28 (1987) 2324–2328.
[31] R. Gregorio Jr., M. Cestari, J. Polym. Sci. B 32 (1994) 859–870.
[32] A. Martinelli, A. Matic, P. Jacobsson, L. Börjesson, M.A. Navarra, S. Panero, B. Scrosati, J. Electrochem. Soc. 154 (2007) G183–G187.
[33] J. Manning, R. Frech, Polymer 33 (1992) 3487–3494.
[34] R. Frech, S. Chintapalli, Solid State Ionics 85 (1996) 61–66.
[35] B. Laik, L. Legrand, A. Chausse, R. Messina, Electrochim. Acta 44 (1998) 773–780.
[36] Z. Wang, M. Ikeda, N. Hirata, M. Kubo, T. Itoh, O. Yamamoto, J. Electrochem. Soc. 146 (1999) 2209–2215.
[37] A. Bernson, J. Lindgren, Polymer 35 (1994) 4842–4847.
[38] M. Egashira, H. Todo, N. Yoshimoto, M. Morita, J. Power Sources 178 (2008) 729.
[39] M. Egashira, H. Shimomura, N. Yoshimoto, M. Morita, J. Yamaki, Electrochemistry 73 (2005) 585.
[40] J. Fan, P.S. Fedkiw, J. Electrochem. Soc. 144 (1997) 399–408.
[41] J. Zhou, P.S. Fedkiw, S.A. Khan, J. Electrochem. Soc. 149 (2002) A1121–A1126.
[42] N. Munichandraiah, G. Sivasankar, L.G. Scanlon, R.A. Marsh, J. Appl. Polym. Sci. 65 (1997) 2191–2199.
[43] N. Munichandraiah, L.G. Scanlon, R.A. Marsh, B. Kumar, A.K. Sircar, J. Appl. Electrochem. 25 (1995) 857–863.
[44] H. Ohno, S. Washiro, M. Yoshizawa, in: Christopher S. Brazel, Robin D. Rogers (Eds.), Ionic Liquids in Polymer Systems, ACS Symposium Series 913, American Chemical Society, Washington, DC, 2005, pp. 89–102.